

# MCMC-driven importance samplers

F. Llorente\*, E. Curbelo\*, L. Martino†, V. Elvira‡, D. Delgado\*

\* Universidad Carlos III de Madrid (UC3M), Spain

† Universidad Rey Juan Carlos (URJC), Spain

‡ University of Edinburgh, UK

May 5, 2021

## Abstract

Monte Carlo methods are the standard procedure for estimating complicated integrals of multidimensional posterior distributions in Bayesian inference. In this work, we focus on LAIS, a class of adaptive importance samplers where Markov chain Monte Carlo (MCMC) algorithms are employed to drive an underlying multiple importance sampling (IS) scheme. Its power lies in the simplicity of the *layered* framework: the *upper layer* locates proposal densities by means of MCMC algorithms, whereas the *lower layer* handles the multiple IS scheme, in order to compute the final estimators. The modular nature of LAIS allows for different possible choices in the upper and lower layers, yielding a variety of different performance and computational costs. In this work, we propose different enhancements in order to increase the efficiency and reduce the computational cost, of both upper and lower layers. The different variants are essential if we aim to address computational challenges arising in real-world applications, such as highly concentrated posterior distributions (due to large amounts of data, etc.). Specifically, Hamiltonian Monte Carlo-driven importance samplers are presented and tested. Furthermore, we introduce different strategies for designing cheaper schemes, for instance, recycling samples generated in the upper layer and using them in the final estimators in the lower layer. Numerical experiments show the benefits of the proposed schemes as compared to a vanilla version of LAIS and other benchmark methods. Related Python and Matlab codes are available at [https://github.com/FLlorente/LAIS\\_extensions](https://github.com/FLlorente/LAIS_extensions).

## 1 Introduction

Bayesian methods have become very popular in statistics, signal processing, and machine learning during the last years and, with them, Monte Carlo (MC) techniques that are often necessary for the implementation of optimal a posteriori estimators [1]-[3]. Indeed, MC methods are powerful tools for numerical inference and optimization [4]-[7].

Markov chain Monte Carlo (MCMC) and importance sampling (IS) are well-known families of MC methods. Since both families have their own drawbacks and benefits, there have been

attempts to combine them in order to design efficient schemes [8]. The Layered Adaptive IS (LAIS) algorithm [8] is one of such attempts, combining the desirable exploratory behavior of MCMC, and the robustness and easier theoretical validation of IS. The main underlying idea of this algorithm is the *layered* (i.e. hierarchical) procedure for generating samples. In order to generate one sample, a location parameter is drawn from a probability density function (pdf)  $\boldsymbol{\mu}' \sim p(\boldsymbol{\mu})$  (that plays the role of a prior pdf over a location parameter in the hierarchical procedure) and, conditionally on it, a sample is generated from some proposal centered at  $\boldsymbol{\mu}'$ , i.e.,  $\mathbf{x}' \sim q(\mathbf{x}|\boldsymbol{\mu}')$ . Then, the sample  $\mathbf{x}'$  is properly weighted according to a *multiple IS* (MIS) procedure [9, 10]. Hence, the *upper layer* is formed by the generation of  $\boldsymbol{\mu}$ 's, while in the *lower layer*, we have the generation of  $\mathbf{x}$ 's and its weighting.

Practical choices of  $p(\boldsymbol{\mu})$  in the upper layer require the use of MCMC algorithms. More generally, more than one MCMC algorithm addressing different  $p_i(\boldsymbol{\mu})$ 's could be used to obtain the location parameters. Therefore, the LAIS framework is flexible and can adopt different configurations. In the upper layer, the user must specify the choices of  $p_i(\boldsymbol{\mu})$  and the MCMC sampling algorithms; in the lower layer, we have to decide the MIS weighting scheme. Although LAIS is quite robust and provides good results in general, some configurations are better than others depending on the context. Moreover, the samples generated in the upper layer are not included in the final estimators.

In this work, we introduce different schemes improving the overall performance and reduce the total computational cost. An optimal theoretical choice of  $p(\boldsymbol{\mu})$  is described jointly with other possible practical choices. For instance, different priors  $p_i(\boldsymbol{\mu})$  can be defined as tempered versions of the posterior in order to foster the exploration of the MCMC chains. We specifically focus on the data-tempered posteriors, that we refer to as *partial posteriors*. Moreover, we can leverage the modular framework of LAIS and use state-of-the-art MCMC algorithms, such as Hamiltonian MC (HMC) and Gibbs sampling (or combination of both), in order to sample  $p(\boldsymbol{\mu})$ . The resulting algorithms are HMC and Gibbs-driven importance samplers, with the additional benefit that an estimator of the marginal likelihood (a.k.a., Bayesian evidence) is also easily provided.

We also discuss different strategies for reducing the overall computational cost. For instance, we propose a procedure for recycling the samples in upper layer and use them in the final estimators, in such a way that the sampling step in the lower layer can even be avoided. This drastically reduces the number of evaluations of the posterior. Moreover, in the lower layer, the cost of weighting can be quite high if we have run long MCMC chains in the upper layer. This problem can also be alleviated by using ideas such as compression or alternative weighting schemes, that reduce the cost but maintain the same performance for the final estimators [11, 12, 13]. We test the variants in different scenarios with synthetic and real data.<sup>1</sup>

## 2 Problem statement

We are interested in making inference about the following vector  $\mathbf{x} = [x_1, \dots, x_{d_x}] \in \mathcal{X}_{\text{tot}} \subseteq \mathbb{R}^{d_x}$ . We receive a set of  $D_Y$  measurements,  $\mathbf{y}_{\text{tot}} = [y_1, y_2, \dots, y_{D_Y}]$ , with each  $y_j \in \mathbb{R}$ ,<sup>2</sup> related to the

<sup>1</sup>Related Python and Matlab codes are available at [https://github.com/FLlorente/LAIS\\_extensions](https://github.com/FLlorente/LAIS_extensions).

<sup>2</sup>We assume  $y_j$  to be scalar only for simplicity.

variable of interest  $\mathbf{x}$ . We denote the complete likelihood function as  $L(\mathbf{y}_{\text{tot}}|\mathbf{x})$ . Considering a prior probability density function (pdf)  $g(\mathbf{x})$ , the *complete posterior* pdf can be written as

$$\bar{\pi}(\mathbf{x}|\mathbf{y}_{\text{tot}}) = \frac{1}{p(\mathbf{y}_{\text{tot}})}L(\mathbf{y}_{\text{tot}}|\mathbf{x})g(\mathbf{x}) = \frac{1}{Z}\pi(\mathbf{x}|\mathbf{y}_{\text{tot}}). \quad (1)$$

where we have denoted  $Z = p(\mathbf{y}_{\text{tot}})$ ,  $\pi(\mathbf{x}|\mathbf{y}_{\text{tot}}) = L(\mathbf{y}_{\text{tot}}|\mathbf{x})g(\mathbf{x})$ .

**Goal.** Our purpose is to make inference about the variable  $\mathbf{x}$  given  $\mathbf{y}_{\text{tot}}$ . For instance, we desire to compute integrals of type

$$\mathbf{I} = \int_{\mathcal{X}_{\text{tot}}} \mathbf{f}(\mathbf{x})\bar{\pi}(\mathbf{x}|\mathbf{y}_{\text{tot}})d\mathbf{x}, \quad (2)$$

where  $\mathbf{f}(\mathbf{x}) : \mathbb{R}^{d_x} \rightarrow \mathbb{R}^s$  and  $\mathbf{I} \in \mathbb{R}^s$  with  $s \geq 1$ . Moreover, we are also interested in the so-called marginal likelihood

$$Z = \int_{\mathcal{X}_{\text{tot}}} \pi(\mathbf{x}|\mathbf{y}_{\text{tot}})d\mathbf{x}. \quad (3)$$

Generally, we are not able to calculate analytically the integrals above. Importance sampling (IS) and Markov chain Monte Carlo (MCMC) are popular Monte Carlo techniques for approximating integrals as in Eq. (2) using samples [1]. IS provides also an estimator of Eq. (3), something that is not straightforward with MCMC (see e.g. [14] for a review of methods for estimating  $Z$ ). In this work, we consider adaptive IS algorithms mixing the benefits of MCMC and IS algorithms [8].

### 3 Layered adaptive importance sampling (LAIS)

LAIS is an adaptive IS framework that consists of two sampling layers (see Table 1).<sup>3</sup> Let  $\{q_{n,0}(\mathbf{x}|\boldsymbol{\mu}_{n,0})\}_{n=1}^N$  denote an initial set of  $N$  parametric proposals. In the upper layer, the location parameters of the proposals are updated by means of MCMC algorithms. In the simplest case, at iteration  $t$ , each  $\boldsymbol{\mu}_{n,t-1}$  independently evolves to  $\boldsymbol{\mu}_{n,t}$  ( $n = 1, \dots, N$ ) by running one iteration of a MCMC algorithm. More generally, the whole population  $\{\boldsymbol{\mu}_{n,t-1}\}_{n=1}^N$  can be updated to  $\{\boldsymbol{\mu}_{n,t}\}_{n=1}^N$ , e.g., considering more sophisticated population MCMC algorithms [15, 16]. Then, after performing  $T$  such iterations, in the lower layer we sample  $\mathbf{x}_{n,t} \sim q_{n,t}(\mathbf{x}|\boldsymbol{\mu}_{n,t})$  for  $n = 1, \dots, N$  and  $t = 1, \dots, T$ , and assign weights for each sample (see Table 2 for different weighting schemes). The *layered* in LAIS amounts to the fact that the adaptation (*upper layer*) is independent from the sampling and weighting steps (*lower layer*). As an example, we can run first, e.g.,  $N$  parallel chains for  $T$  iterations each in order to obtain the  $NT$  location parameters  $\{\boldsymbol{\mu}_{n,t}\}$ , and then perform standard IS with the  $NT$  proposals. The weighting procedure is done according to the so-called *deterministic mixture* approach [9, 10]. Some possible choices of the denominator of the importance weights are given in Table 2. Clearly, in the special case of a unique chain  $N = 1$ ,

<sup>3</sup>The code of standard LAIS is also available at [https://github.com/FLlorente/LAIS\\_extensions](https://github.com/FLlorente/LAIS_extensions).

the spatial denominator becomes the standard IS denominator. If  $N$  single MCMC steps are performed, i.e.,  $T = 1$ , then the temporal denominator becomes the standard IS denominator.

The estimators of Eq. (2) and Eq. (3) are then given by

$$\widehat{Z} = \frac{1}{NT} \sum_{t=1}^T \sum_{n=1}^N w_{n,t}, \quad (4)$$

$$\widehat{\mathbf{I}} = \frac{1}{NT\widehat{Z}} \sum_{n=1}^N \sum_{t=1}^T w_{n,t} \mathbf{f}(\mathbf{x}_{n,t}). \quad (5)$$

Table 1: LAIS algorithm

Choose  $\{q_{n,0}\}_{n=1}^N$ ,  $\{\boldsymbol{\mu}_{n,0}\}_{n=1}^N$  and the MCMC algorithms in the upper layer.

**Upper layer (MCMC).**

- **Adaptation:** Apply MCMC transitions with invariant pdf  $p_n(\boldsymbol{\mu})$ , e.g.,  $p_n(\boldsymbol{\mu}) = \bar{\pi}(\boldsymbol{\mu}|\mathbf{y}_{\text{tot}})$ , i.e.,

$$\{\boldsymbol{\mu}_{n,t-1}\}_{n=1}^N \xrightarrow{\text{MCMC}} \{\boldsymbol{\mu}_{n,t}\}_{n=1}^N, \quad \forall t = 1, \dots, T.$$

**Lower layer (IS).**

- **Sampling:**  $\mathbf{x}_{n,t} \sim q_{n,t}(\mathbf{x}|\boldsymbol{\mu}_{n,t})$ , for all  $n, t$ .
- **Weighting:**

$$w_{n,t} = \frac{\pi(\mathbf{x}_{n,t}|\mathbf{y}_{\text{tot}})}{\boldsymbol{\Phi}(\mathbf{x}_{n,t})}, \quad \forall n, t, \quad (6)$$

where different denominators,  $\boldsymbol{\Phi}(\mathbf{x}_{n,t})$ , are possible. See Table 2.

**Consistency.** LAIS can be interpreted as a standard, static IS scheme with  $NT$  proposals, and the consistency only depends on the proper choice of the denominator  $\boldsymbol{\Phi}(\mathbf{x})$  in the importance weights. In Table 2, some proper choices are provided which follows the deterministic mixture approach [9, 10]. It is important to remark that the consistency does not depend on the choice of the densities  $p_n(\boldsymbol{\mu})$  in the upper layer but, clearly, the efficiency of LAIS is affected by the selected pdfs  $p_n(\boldsymbol{\mu})$ .

**Evaluations of the posterior.** In the standard LAIS implementation (i.e. setting  $p_n(\boldsymbol{\mu}) = \bar{\pi}(\boldsymbol{\mu}|\mathbf{y}_{\text{tot}})$  for all  $n$ ), the total number of evaluations  $E$  of the posterior is  $E = 2NT$ , where  $NT$  evaluations are performed in the upper layer and  $NT$  in the lower layer. However, the final estimators only involve  $S = NT$  samples.

Table 2: Possible denominators  $\Phi(\mathbf{x}_{n,t})$ .

complete	temporal	spatial	standard
$\frac{1}{NT} \sum_{\tau=1}^T \sum_{i=1}^N q_{i,\tau}(\mathbf{x}_{n,t} \boldsymbol{\mu}_{i,\tau})$	$\frac{1}{T} \sum_{\tau=1}^T q_{n,\tau}(\mathbf{x}_{n,t} \boldsymbol{\mu}_{n,\tau})$	$\frac{1}{N} \sum_{i=1}^N q_{i,t}(\mathbf{x}_{n,t} \boldsymbol{\mu}_{i,t})$	$q_{n,t}(\mathbf{x}_{n,t} \boldsymbol{\mu}_{n,t})$

**Denominators.** The computation of the weights in the lower layer allows for different possible denominators, shown in Table 2. The function  $\Phi(\mathbf{x}_{n,t})$  can be taken to be the proposal that actually generated  $\mathbf{x}_{n,t}$  (*standard*), the mixture of proposals across different chains (*spatial*), the mixture of proposals within the chain (*temporal*), or the mixture of all proposals (*complete*). Note that, we always have the evaluation of the complete posterior in the numerator, hence all the weighting strategies have the same number of posterior evaluations, i.e.,  $NT$ . However, in practice, the cost of the *complete*, *temporal* and *spatial* weighting schemes is higher than the *standard* one, and it will increase the overall computation time. This is more obvious in real applications where many chains are run for a long time, i.e.,  $T$  and  $N$  are very large. Commonly,  $T \gg N$ , so that the *spatial* scheme is cheaper than the *temporal* scheme, and both are much cheaper than the *complete* scheme. In return, these schemes can produce a huge improvement in the performance of the final estimators. Indeed, our experiments show that the *complete* scheme consistently produces more stable estimators with only a small increase in computational cost, as compared to the overall cost of the algorithm.

**Elements in LAIS.** It is important to note that a specific implementation of LAIS is determined by the choices of

- the invariant densities  $p_n(\boldsymbol{\mu})$ ,
- the MCMC approach (e.g. parallel or single longer chain Metropolis-Hastings, advanced MCMC schemes, etc.),
- the proposals  $q_{n,t}(\mathbf{x}|\boldsymbol{\mu}_{n,t})$ , and
- the denominator  $\Phi(\mathbf{x})$ .

By setting each of these elements, we define a specific LAIS implementation. Below, we discuss some important theoretical considerations and, at the same time, we present several variants and improvements for the LAIS framework concerning each one of the elements above. For instance, regarding the pdfs  $p_n(\boldsymbol{\mu})$ , we describe the suitable use of different type of tempered posteriors. The application of sophisticated MCMC algorithms in the upper layer is also discussed. Recycling sample schemes (which involve the selection of proposals  $q_{n,t}$  as well) and the design of cheaper denominators in the lower layer are also introduced.

## 4 Choice of the invariant density $p(\boldsymbol{\mu})$ in the upper layer

In this section, we provide important considerations and, then we introduce novel schemes. First, we provide a theoretical discussion regarding the optimal choice of the upper layer density  $p(\boldsymbol{\mu})$ . This discussion clarifies the flexibility in the upper layer design, and justifies even the possible use of anti-tempered posteriors as well. An improved version of LAIS that makes use of partial posteriors in the upper layer is also presented.

### 4.1 Optimal density in upper layer

Let us consider a simplified hierarchical procedure which mimics the LAIS sample generation approach. For this purpose, we consider a single proposal pdf  $q$  in the lower layer defined by the mean  $\boldsymbol{\mu} \in \mathbb{R}^{d_x}$  and scale matrix  $\mathbf{C} \in \mathbb{R}^{d_x \times d_x}$ , so that the proposal can be denoted as  $q(\mathbf{x}|\boldsymbol{\mu}, \mathbf{C})$ , and it fulfills  $q(\mathbf{x}|\boldsymbol{\mu}, \mathbf{C}) = q(\mathbf{x} - \boldsymbol{\mu}|\mathbf{0}, \mathbf{C})$ .<sup>4</sup> We assume that the location parameter  $\boldsymbol{\mu}$  is drawn exactly from the density  $p(\boldsymbol{\mu})$ .<sup>5</sup> Hence, the simplified LAIS generation procedure is given below:

1. Draw a possible location parameter  $\boldsymbol{\mu}' \sim p(\boldsymbol{\mu})$ .
2. Draw  $\mathbf{x} \sim q(\mathbf{x}|\boldsymbol{\mu}', \mathbf{C})$ .

Note that  $p(\boldsymbol{\mu})$  plays the role of a prior pdf over the location parameter of  $q$ . The sample  $\mathbf{x}$  is distributed according to the following equivalent density,

$$\tilde{q}(\mathbf{x}|\mathbf{C}) = \int_{\mathcal{X}} q(\mathbf{x}|\boldsymbol{\mu}, \mathbf{C})p(\boldsymbol{\mu})d\boldsymbol{\mu} = \int_{\mathcal{X}} q(\mathbf{x} - \boldsymbol{\mu}|\mathbf{0}, \mathbf{C})p(\boldsymbol{\mu})d\boldsymbol{\mu}, \quad (7)$$

i.e.,  $\mathbf{x} \sim \tilde{q}(\mathbf{x}|\mathbf{C})$ . From Eqs. (7) and (9) we can deduce the following considerations. The last expression in (7) is a convolution integral. Hence, considering the sum of two independent random variables

$$\mathbf{X} = \mathbf{Z} + \mathbf{M}, \quad (8)$$

where  $\mathbf{Z} \sim q(\mathbf{x}|\mathbf{0}, \mathbf{C})$  (with  $\boldsymbol{\mu} = \mathbf{0}$ ) and  $\mathbf{M} \sim p(\boldsymbol{\mu})$ , then  $\mathbf{X}$  is distributed as  $\tilde{q}(\mathbf{x}|\mathbf{C})$  [1].

Now, we consider the problem of finding the optimal density  $p^*(\boldsymbol{\mu}|\mathbf{C})$  over the location parameter  $\boldsymbol{\mu}$ . In LAIS, the samples obtained by this procedure are then used in a self-normalized importance estimator. The variance of the IS weights is minimized when the proposal is exactly  $\bar{\pi}(\mathbf{x}|\mathbf{y}_{\text{tot}})$  (e.g. see [17]). Therefore, the desirable scenario is to have  $\tilde{q}(\mathbf{x}|\mathbf{C}) = \bar{\pi}(\mathbf{x}|\mathbf{y}_{\text{tot}})$ . The optimal pdf depends on the chosen scale parameter  $\mathbf{C}$  and since  $q(\mathbf{x}|\boldsymbol{\mu}, \mathbf{C}) = q(\mathbf{x} - \boldsymbol{\mu}|\mathbf{0}, \mathbf{C})$ , as  $\boldsymbol{\mu}$  is a location parameter, we can write

$$\bar{\pi}(\mathbf{x}|\mathbf{y}_{\text{tot}}) = \int_{\mathcal{X}} q(\mathbf{x} - \boldsymbol{\mu}|\mathbf{0}, \mathbf{C})p^*(\boldsymbol{\mu}|\mathbf{C})d\boldsymbol{\mu}. \quad (9)$$

Equation (9) above can be rewritten in terms of the characteristic functions:  $Q(\boldsymbol{\nu}|\mathbf{C}) = E \left[ q(\mathbf{x}|\mathbf{0}, \mathbf{C})e^{i\boldsymbol{\nu}^\top \mathbf{x}} \right]$ ,  $P^*(\boldsymbol{\nu}|\mathbf{C}) = E \left[ p^*(\boldsymbol{\mu}|\mathbf{C})e^{i\boldsymbol{\nu}^\top \boldsymbol{\mu}} \right]$ , and  $\Pi(\boldsymbol{\nu}) = E \left[ \bar{\pi}(\mathbf{x}|\mathbf{y}_{\text{tot}})e^{i\boldsymbol{\nu}^\top \mathbf{x}} \right]$ , where  $\boldsymbol{\nu} \in$

<sup>4</sup>This property is satisfied by relevant distributions such as Gaussian, Student's t and Laplace.

<sup>5</sup>This is clearly a simplification since, with MCMC chains, we obtain correlated samples.

$\mathbb{R}^{d_x}$ . The characteristic function of  $\mathbf{X}$  is the product of characteristic functions of  $\mathbf{Z}$  and  $\mathbf{M}$ . Hence, the optimal pdf in the upper layer has the following characteristic function,

$$P^*(\boldsymbol{\nu}|\mathbf{C}) = \frac{\bar{\Pi}(\boldsymbol{\nu})}{Q(\boldsymbol{\nu}|\mathbf{C})}. \quad (10)$$

In a general case, it is not possible to determine analytically the expression of the optimal pdf  $p^*(\boldsymbol{\mu}|\mathbf{C})$ , and thus, other practical choices must be considered, as discussed below.

## 4.2 Practical choices

Here, we discuss some practical selection of  $p(\boldsymbol{\mu})$ . First of all, from Eq. (8), we can obtain the following relevant considerations for this purpose:

1.  $E[\mathbf{X}] = E[\mathbf{Z}] + E[\mathbf{M}] = 0 + E[\mathbf{M}]$ , i.e., the expected value of the equivalent proposal  $\tilde{q}$  is equal to the expected value of the density  $p(\boldsymbol{\mu})$  in the upper layer.
2.  $\text{Var}[\mathbf{X}] = \text{Var}[\mathbf{Z}] + \text{Var}[\mathbf{M}] \geq \text{Var}[\mathbf{M}]$ , where  $\text{Var}[\cdot]$  returns the elements in the diagonal of the covariance matrix and, the inequality  $\geq$  is applied to each element in the diagonal. Namely, the variances of each component of the equivalent proposal  $\tilde{q}$  are greater or equal to the variances of each component of the density  $p(\boldsymbol{\mu})$  in the upper layer.

Thus, the equivalent density  $\tilde{q}(\mathbf{x}|\mathbf{C})$  has the same expected value and a bigger variance with respect to the density  $p(\boldsymbol{\mu})$ .

**Consideration about the optimal pdf  $p^*(\boldsymbol{\mu})$ .** Given Eq. (9) and the observations above, we can deduce that the optimal pdf  $p^*(\boldsymbol{\mu})$  will have the same mean as the posterior, and it will have lighter tails than the posterior  $\bar{\pi}$  (i.e.,  $p^*$  is more “concentrated” than  $\bar{\pi}$ ).

**A possible choice of  $p(\boldsymbol{\mu})$  in the upper layer.** In practice, we cannot employ the optimal  $p^*(\boldsymbol{\mu})$ . However, the choice  $p(\boldsymbol{\mu}) = \bar{\pi}(\boldsymbol{\mu}|\mathbf{y}_{\text{tot}})$  provides an equivalent proposal with the same mean as the posterior, but with heavier tails. This is a good property: indeed, it avoids infinite variance estimators (see Example 1 in [14]) and this is the reason why this choice works well in practice [8]. It can be shown that, in this case, the equivalent proposal is the kernel density estimator of the posterior (for a fixed optimal choice of  $\mathbf{C}$ ). However, when there are large amounts of data, evaluating the posterior can be very costly, so that the upper layer can require too much computational time. Furthermore, it is common that  $\pi(\mathbf{x}|\mathbf{y}_{\text{tot}})$  is highly concentrated in some regions, so the MCMC algorithms in the upper layer can suffer from bad mixing. Also in this scenario, LAIS is able to provide final consistent estimators due to the use of weighted samples in the lower layer.

### 4.2.1 Standard Tempering and anti-tempering

One idea for solving the second issue above, i.e., the bad mixing of the MCMC chains when  $\pi(\mathbf{x}|\mathbf{y}_{\text{tot}})$  is highly concentrated, is the so-called *tempering*. Roughly speaking, tempering is

a technique used to artificially change the scale of the target density. It is commonly used in order to improve the exploration of the posterior support in optimization, MCMC and IS [18, 19]. For instance, taking  $p(\boldsymbol{\mu}) \propto [\pi(\boldsymbol{\mu}|\mathbf{y}_{\text{tot}})]^\beta$  with  $0 < \beta < 1$  as the target density can be useful if  $\bar{\pi}$  concentrates in a small region that is not easy to discover. The  $\beta$  is usually referred to as the (inverse) temperature parameter. More generally, a temperature schedule is a sequence of tempered posteriors ending with  $\bar{\pi}$ . A common choice is the geometric path between prior and posterior  $\bar{\pi}_{\beta_n}(\mathbf{x}|\mathbf{y}_{\text{tot}}) \propto \pi(\mathbf{x}|\mathbf{y}_{\text{tot}})^{\beta_n} g(\mathbf{x})^{1-\beta_n} = L(\mathbf{y}_{\text{tot}}|\mathbf{x})^{\beta_n} g(\mathbf{x})$ , for a sequence  $0 = \beta_0 < \beta_1 < \dots < \beta_N = 1$ , such  $\bar{\pi}_{\beta_0}(\mathbf{x}|\mathbf{y}_{\text{tot}}) = g(\mathbf{x})$  (i.e., the prior pdf over  $\mathbf{x}$ ) and  $\bar{\pi}_{\beta_N}(\mathbf{x}|\mathbf{y}_{\text{tot}}) = \bar{\pi}(\mathbf{x}|\mathbf{y}_{\text{tot}})$ . Note that the tempered posterior has a powered, less informative (i.e., wider) likelihood.

Therefore, in order to improve the exploration of the posterior support, one possibility consists in taking  $p_n(\boldsymbol{\mu}) = \bar{\pi}_{\beta_n}(\mathbf{x}|\mathbf{y}_{\text{tot}})$  in the upper layer.

**Anti-tempering.** An important point to remark that, in LAIS, we can have  $\beta \leq 1$  in order to foster the mixing of the chains, but also we can choose some  $\beta > 1$  since, theoretically, the optimal pdf  $p^*(\boldsymbol{\mu})$  is more “concentrated” than the posterior  $\bar{\pi}$  (as we have seen above).

In any case, with a standard tempering strategy (using an auxiliary parameter  $\beta$ ), we only solve one of the two issues pointed out in the previous section: improving the exploration of the posterior support. The cost of evaluating a tempered posterior  $\bar{\pi}_{\beta_n}(\mathbf{x})$  is the same as the cost of evaluating the non-tempered posterior  $\bar{\pi}$ . An alternative to the standard tempering procedure is the so-called *data tempering*, which reduces also the evaluation cost.

#### 4.2.2 Data tempering and partial posteriors

Let  $\mathbf{y}_n \in \mathbb{R}^{K_n}$  denote a subset of data points, i.e.,  $\mathbf{y}_n \subset \mathbf{y}_{\text{tot}}$  (with  $K_n \ll D_Y$ ) and assume we have  $N$  subsets  $\mathbf{y}_1, \dots, \mathbf{y}_N$ . These  $\mathbf{y}_n$  can represent a partition  $\mathbf{y}_{\text{tot}}$  in  $N$  non-overlapping pieces so that  $\sum_{n=1}^N K_n = D$ , but in general we could have  $\mathbf{y}_n \cap \mathbf{y}_{n'} \neq \emptyset$ . We can define the *partial posteriors* and use them as invariant densities in the upper layer,

$$p_n(\mathbf{x}) = \bar{\pi}_n(\mathbf{x}|\mathbf{y}_n) \propto L_n(\mathbf{y}_n|\mathbf{x})g_n(\mathbf{x}), \quad (11)$$

where  $L_n(\mathbf{y}_n|\mathbf{x})$  is the likelihood of the batch  $\mathbf{y}_n$ , and  $g_n(\mathbf{x})$  plays the role of a partial prior pdf. For our purpose, we can keep  $g_n(\mathbf{x}) = g(\mathbf{x})$  for all  $n$ , or we can split the prior contribution into each data subset, for instance, setting  $g_n(\mathbf{x}) = g(\mathbf{x})^{\frac{1}{N}}$  for all  $n$ , which is a typical choice in the Big Data context [20, 21]. Therefore, the partial posterior  $\bar{\pi}_n$  is a tempered version of the posterior since its likelihood  $L_n(\mathbf{y}_n|\mathbf{x})$  is less informative, i.e. hence wider, than in the case where we consider all data.

Thus, we consider that each MCMC chain in the upper layer addresses a different partial posterior  $p_n(\mathbf{x}) = \bar{\pi}_n(\mathbf{x}|\mathbf{y}_n)$  ( $n = 1, \dots, N$ ). Hence, there are as many chains as number of partial posteriors. We call this scheme as *Partial posteriors LAIS* (PLAIS) method. Note that, in PLAIS, we still evaluate the complete posterior in the lower layer, so the total number of full posterior evaluations is  $NT$  (in the lower layer).

Hence, the motivation and benefits of PLAIS are twofold: (i) the cost of the upper layer gets reduced since each chain works only with a subset of the data, and (ii) using the partial posteriors, we have a tempered effect which fosters the exploration of the MCMC chains. Moreover, the use

of partial posteriors produces more dispersed location parameters of the proposals in the lower layer. This increases the robustness of the method, since it reduces the chance of obtaining huge weights and, as a consequence, avoids IS estimators with infinite variance (see Example 1 in [14]).

## 5 Advanced schemes in the upper layer

The simplest choice of MCMC schemes in the upper layer is to consider  $N$  independent MH algorithms. However, more sophisticated algorithms can be considered (such as Langevin, Hamiltonian and Gibbs samplers), which can further enhance the performance of the algorithm. On the other hand, the LAIS approach can be interpreted as a way to help these MCMC schemes to improve the efficiency of their estimators and allow them to estimate efficiently the marginal likelihood  $Z$ . We also discuss a way to summarize the information in the upper layer in order to reduce the cost of the lower layer.

### 5.1 Hamiltonian and Gibbs-driven importance samplers

**Hamiltonian MC in the upper layer.** The Hamiltonian Monte Carlo (HMC) algorithm is usually considered as the state-of-the-art technique in the MCMC world. However, as with the rest of MCMC methods, it is not straightforward to estimate the marginal likelihood with HMC samples [14]. Additionally, it is well-known the difficulty of tuning its hyperparameters for obtaining efficient sampling [22]. In this context, we propose using different HMC algorithms in the upper layer in Table 1, each chain employing possibly different parameters. Thus, several sets of parameters are jointly used. Note also that we do not need to fine-tune the hyperparameters since the states in the upper layer are not used directly as samples in our framework. The lower layer in LAIS provides a straightforward estimation of the marginal likelihood. We compare the performance of these algorithms, which call HMC-LAIS, with HMC in Sect. 8.2.

**Gibbs algorithms in the upper layer.** Another possibility is to use Gibbs samplers in the upper layer [1]. Considering the use of full-conditionals, the Gibbs sampler can be slow since it is a component-wise scheme, i.e., each component of the parameter vector  $\mathbf{x}$  is drawn from the corresponding full-conditional keeping fixed the rest of components. However, they have the advantage of working in lower dimension, which allows for designing more efficient samplers in high dimensional spaces. For instance, extremely efficient MH-within-Gibbs algorithms can be designed using Adaptive Rejection Metropolis schemes for drawing from each one-dimensional full-conditional [23, 24, 25, 26]. Other possibility is to employ the adaptive direction sampling which can speed up the mixing of Gibbs chains, choosing different one-dimensional direction of sampling at each iteration [27].

More generally, the joint use of HMC, Langevin and Gibbs-based schemes can be potential applied in the upper layer. The advantages of each MCMC algorithm are then combined and the final weighted samples in the lower layer can perform a consistent estimation of the marginal likelihood, also in this scenario.

## 5.2 Compression for a cheap sampling and weighting

As we have commented before, the *complete* weighting scheme (see Table 2) provides the best performance in terms of variance, at the expense of an increase in the computational cost, specially in real applications since  $T$  and  $N$  can be very large. One possibility in order to reduce this cost, without decreasing  $T$  or  $N$ , is the use of partial MIS denominators [9, 11]. Another possibility consists in using some technique that summarizes the population of  $NT$  samples. For instance, to apply a compression of Monte Carlo samples [12], as we describe below. These schemes reduces the cost of both sampling and weighting in the lower layer.

**Compressed LAIS (CLAIS).** Let consider a set of  $R$  means  $\{\boldsymbol{\mu}_k\}_{k=1}^R$  generated by MCMC in the upper layer, and let  $M$  be a constant value such that  $M < R$ . Note that, in the case of  $N$  parallel chains of length  $T$  in the upper layer, we have  $R = NT$ . Given a partition of  $\mathcal{X}_{\text{tot}}$ , i.e.,  $\mathcal{X}_1 \cup \mathcal{X}_2 \cup \dots \cup \mathcal{X}_M = \mathcal{X}_{\text{tot}}$  formed by convex, disjoint sub-regions  $\mathcal{X}_m$ , we denote the subset of the set of indices  $\{1, \dots, R\}$ ,

$$\mathcal{J}_m = \{i = 1, \dots, R : \boldsymbol{\mu}_i \in \mathcal{X}_m\},$$

which are associated with the samples in the  $m$ -th sub-region  $\mathcal{X}_m$ . The cardinality  $|\mathcal{J}_m|$  denotes the number of samples in  $\mathcal{X}_m$  and we have  $\sum_{m=1}^M |\mathcal{J}_m| = R$ . We can compress the information contained in samples, constructing a stratified approximation based on  $M$  weighted particles  $\{\mathbf{s}_m, a_m\}_{m=1}^M$ , where  $\mathbf{s}_m$  is a (properly chosen) point in  $\mathcal{X}_m$  and  $a_m = \frac{|\mathcal{J}_m|}{R}$ . The summary points  $\mathbf{s}_m$  can be randomly chosen, picking uniformly a mean in  $\mathcal{X}_m$ , in the set  $\{\boldsymbol{\mu}_i\}_{i \in \mathcal{J}_m}$  or using a deterministic procedure, e.g.,

$$\mathbf{s}_m = \frac{1}{|\mathcal{J}_m|} \sum_{j \in \mathcal{J}_m} \boldsymbol{\mu}_j. \quad (12)$$

For the statistical properties of these choices see [12]. Other choices based on empirical quantiles are also possible. As an example, a suitable compression scheme can be provided applying a clustering method to the set  $\{\boldsymbol{\mu}_k\}_{k=1}^R$ , where  $M$  represents the number of clusters. After the compression, we can consider as proposal and denominator in the lower layer the following Gaussian mixture,<sup>6</sup>

$$q_M(\mathbf{x}) = \sum_{m=1}^M a_m \mathcal{N}(\mathbf{x} | \mathbf{s}_m, \boldsymbol{\Sigma}). \quad (13)$$

Thus, the mixture  $q_M$  is used for sampling and computing the weights in the lower layer. The  $d_x \times d_x$  covariance matrix  $\boldsymbol{\Sigma}$  is obtained as

$$\boldsymbol{\Sigma} = \mathbf{Q}_\mu - \mathbf{Q}_C + \sigma_p^2 \mathbf{I}. \quad (14)$$

where  $\mathbf{Q}_\mu = \frac{1}{R} \sum_{k=1}^R (\boldsymbol{\mu}_k - \mathbf{m})(\boldsymbol{\mu}_k - \mathbf{m})^\top$  with  $\mathbf{m} = \frac{1}{R} \sum_{k=1}^R \boldsymbol{\mu}_k$  is the covariance matrix of all  $R$  means  $\boldsymbol{\mu}_k$ , and  $\mathbf{Q}_C = \sum_{m=1}^M a_m (\mathbf{s}_m - \mathbf{m}_C)(\mathbf{s}_m - \mathbf{m}_C)^\top$  with  $\mathbf{m}_C = \sum_{m=1}^M a_m \mathbf{s}_m$  is the covariance matrix of the summary samples.<sup>7</sup> Finally,  $\mathbf{I}$  is a unit matrix, and  $\sigma_p^2$  is chosen by the user. With

<sup>6</sup>Clearly, other type of mixture can be employed, e.g., a t-Student mixture.

<sup>7</sup>Clearly, if  $\mathbf{s}_m$  are chosen as in Eq. (12), then  $\mathbf{m} = \mathbf{m}_C$ .

$\mathbf{s}_m$  in Eq. (12), it is possible to show that

$$\mathbf{Q}_\mu - \mathbf{Q}_C = \sum_{m=1}^M a_m \left( \frac{1}{|\mathcal{J}_m|} \sum_{j \in \mathcal{J}_m} (\boldsymbol{\mu}_j - \mathbf{s}_m) (\boldsymbol{\mu}_j - \mathbf{s}_m)^\top \right). \quad (15)$$

That is, the covariance of each component in  $q_M$  is the weighted average of the covariances within clusters plus the term  $\sigma_p^2 \mathbf{I}$ . The choice of  $\mathbf{s}_m$  in Eq. (12) has the following property. Let us assume that, without compression, we would like to use proposals  $q$  in the lower layer with a covariance matrix  $\sigma_p^2 \mathbf{I}$ . Without compression, we have  $M = R$ ,  $\mathbf{s}_k = \boldsymbol{\mu}_k$ ,  $\mathbf{Q}_\mu = \mathbf{Q}_C$ , so we have the covariance of each mixture component is  $\boldsymbol{\Sigma} = \sigma_p^2 \mathbf{I}$ , as expected. With the maximum compression,  $M = 1$ , then  $\mathbf{Q}_C$  is null and  $\boldsymbol{\Sigma} = \mathbf{Q}_\mu + \sigma_p^2 \mathbf{I}$ . Hence, with maximum compression, the proposal  $q_M$  takes into account the dispersion set by the user plus the covariance matrix of the  $R$  means  $\boldsymbol{\mu}_k$ , obtained in the upper layer. Note that, clearly, the cost of the employed compression technique must be lower than the cost of evaluating the full denominator. We have tested the performance of CLAIS with several choices of  $R$ , and compared it against LAIS in Section 8.2.

## 6 Recycling LAIS (RLAIS)

In this Section, we discuss the possibility of recycling the samples, and their corresponding evaluations, from the upper layer for their use in the lower layer, hence reducing the overall computational cost. For simplicity, let us assume the use of  $N$  parallel Metropolis-Hastings (MH) algorithms in the upper layer. Moreover, in this first part of the section, assume that  $p_n = \bar{\pi}$  for all  $n$ . Given the initial state  $\boldsymbol{\mu}_{n,0}$ , a proposal pdf  $\varphi_n$ , and a length value  $T$ , The  $n$ -th MH chain follows the following steps:

- **For**  $t = 1, \dots, T$ :

1. Draw  $\mathbf{z}_{n,t} \sim \varphi_n(\mathbf{x} | \boldsymbol{\mu}_{n,t-1})$ .
2. Set  $\boldsymbol{\mu}_{n,t} = \mathbf{z}_{n,t}$  with probability

$$\alpha = \min \left[ 1, \frac{\pi(\mathbf{z}_{n,t} | \mathbf{y}_{\text{tot}}) \varphi_n(\boldsymbol{\mu}_{n,t-1} | \mathbf{z}_{n,t})}{\pi(\boldsymbol{\mu}_{n,t-1} | \mathbf{y}_{\text{tot}}) \varphi_n(\mathbf{z}_{n,t} | \boldsymbol{\mu}_{n,t-1})} \right], \quad (16)$$

otherwise, set  $\boldsymbol{\mu}_{n,t} = \boldsymbol{\mu}_{n,t-1}$  (with probability  $1 - \alpha$ ).

- **Outputs:** The chain  $\{\boldsymbol{\mu}_{n,t}\}_{t=1}^T$ . Additionally, we obtain and store  $\{\mathbf{z}_{n,t}\}_{t=1}^T$ ,  $\{\pi(\mathbf{z}_{n,t} | \mathbf{y}_{\text{tot}})\}_{t=1}^T$  and  $\{\varphi_n(\mathbf{z}_{n,t} | \boldsymbol{\mu}_{n,t-1})\}_{t=1}^T$ .

Therefore, at each iteration, a candidate is drawn  $\mathbf{z}_{n,t} \sim \varphi_n(\mathbf{x} | \boldsymbol{\mu}_{n,t-1})$  and then it is tested (accepted or discarded) as possible new state, according to the acceptance MH probability. If we store all candidates  $\{\mathbf{z}_{n,t}\}_{t=1}^T$  and the corresponding evaluations of the posterior  $\{\pi(\mathbf{z}_{n,t} | \mathbf{y}_{\text{tot}})\}_{t=1}^T$  (for all  $n$ ), required in the computation of  $\alpha$  in Eq. (16), we can use them in the lower layer as samples, i.e., we set  $\mathbf{x}_{n,t} = \mathbf{z}_{n,t}$ . In this way, we reduce the computation time since we do not need

to draw additional samples.

Note that  $\varphi_n(\mathbf{x}|\boldsymbol{\mu}_{n,t-1})$  becomes the proposal in the lower layer, i.e., we set  $q_{n,t}(\mathbf{x}) = \varphi_n(\mathbf{x}|\boldsymbol{\mu}_{n,t-1})$ . The evaluations of the proposal  $\varphi_n(\mathbf{z}_{n,t}|\boldsymbol{\mu}_{n,t-1})$  can be also stored. Depending on the choice of the weighting scheme in the lower layer, other evaluations of different proposals  $\varphi_j$ , with  $j \neq n$  can be required. The algorithm is outlined in Table 3, and Table 4 shows different weighting procedures. Since  $p_n = \bar{\pi}$  and the posterior evaluations are recycled, the total number of posterior evaluations in RLAIS is only  $E = NT$ .

**Consistency.** It is important to note that we can find an equivalent proposal  $\tilde{q}_{MH}(\mathbf{x})$  of MH-type algorithms which can be expressed as a convolution integral, similarly as we have done in LAIS. See the Appendix A for more details. In RLAIS, the different MIS denominators can be considered as Monte Carlo approximations of this equivalent proposal  $\tilde{q}_{MH}$  expressed as the integral in Eq. (29). Therefore, in the case of the first 3 different MIS denominators (the complete, spatial and temporal mixtures) as  $N$  and  $T$  grow, the chosen denominator provides an better approximation of the  $\tilde{q}_{MH}$  and the MIS weights becomes closer and closer to standard importance weights of the form  $w_{n,t} = \frac{\pi(\mathbf{x}_{n,t}|\mathbf{y}_{\text{tot}})}{\tilde{q}_{MH}(\mathbf{x}_{n,t})}$ . RLAIS can be seen as a multiple-chain generalization of [28, 29].

Table 3: LAIS with recycling of samples (RLAIS)

1. **Sampling:** Let consider Metropolis-Hastings (MH)-type schemes with random walk proposal densities  $\varphi_{n,t}(\mathbf{x}|\boldsymbol{\mu}_{n,t})$  ( $\varphi_{n,t}$  can vary with  $t$  since we assume they can be also adaptive schemes), generating  $N$  MCMC chains of length  $T$ .

Then, the states of the chains are  $\boldsymbol{\mu}_{n,t}$ , for  $n = 1, \dots, N$  and  $t = 1, \dots, T$ . At each iteration of one MH scheme, we draw a candidate  $\mathbf{z}_{n,t} \sim \varphi_{n,t}(\mathbf{x}|\boldsymbol{\mu}_{n,t-1})$  that will be accepted or rejected in the MH step. We save all the  $NT$  candidates  $\mathbf{z}_{n,t}$  for  $n = 1, \dots, N$  and  $t = 1, \dots, T$ .

2. **Weighting:** Assign to  $\mathbf{z}_{n,t}$  the weights

$$w_{n,t} = \frac{\pi(\mathbf{z}_{n,t}|\mathbf{y}_{\text{tot}})}{\boldsymbol{\Psi}(\mathbf{z}_{n,t})}, \quad (17)$$

where different possible choices for  $\boldsymbol{\Psi}(\mathbf{z}_{n,t})$  are possible (see Table 4).

3. **Output:** Return all the pairs  $\{\mathbf{z}_{n,t}, w_{n,t}\}$ , and/or the estimators given in Eqs (4) and (5).

**PLAIS with recycling (PA-RLAIS).** We can combine the idea of using the partial posteriors and the RLAIS approach. Indeed, also in PLAIS, it is possible to avoid the sampling step if we recycle all candidates produced within the MH algorithms in the upper layer. We denote the resulting scheme as PA-RLAIS. We can recycle the candidates  $\{\mathbf{z}_{n,t}\}_{t=1}^T$  and the proposal evaluations  $\{\varphi_n(\mathbf{z}_{n,t}|\boldsymbol{\mu}_{n,t-1})\}_{t=1}^T$  (for all  $n$ ) but, in this scenario, we have not evaluations of the full posterior in the upper layer (then we cannot recycle the posterior evaluations).

Table 4: Possible denominators  $\Psi(\mathbf{x}_{n,t})$ .

complete	temporal	spatial	standard
$\frac{1}{NT} \sum_{\tau=0}^{T-1} \sum_{n=1}^N \varphi_{n,\tau}(\mathbf{x}_{n,t} \boldsymbol{\mu}_{n,\tau})$	$\frac{1}{T} \sum_{\tau=0}^{T-1} \varphi_{n,\tau}(\mathbf{x}_{n,t} \boldsymbol{\mu}_{n,\tau})$	$\frac{1}{N} \sum_{n=1}^N \varphi_{n,t}(\mathbf{x}_{n,t} \boldsymbol{\mu}_{n,t})$	$\varphi_{n,t}(\mathbf{x}_{n,t} \boldsymbol{\mu}_{n,t})$

## 6.1 Summary of the computation costs of the proposed schemes

Generally, the most costly step is the evaluation of the complete posterior  $\pi(\mathbf{x}|\mathbf{y}_{\text{tot}})$  (due to a costly model or number of data). The evaluation of the partial posteriors is not that costly since we choose the batch sizes such  $K_n \ll D_Y$  for all  $n = 1, \dots, N$ . Thus, the comparison among PLAIS, RLAIS and PAPIS, as well as with other methods, must be done in terms of number of evaluations of  $\pi$ . In this sense, PLAIS, and RLAIS have the same cost of  $NT$  evaluations of  $\pi$  (with the same choice of  $N$  and  $T$  for the three algorithms). RLAIS is less costly than PLAIS since the formers do not need additional samples. A summary of the number of evaluations of  $\pi$  and all partial posteriors  $\pi_n$ 's is given below:

Method	Upper layer		Lower layer	Drawing samples
	evals of $\pi(\mathbf{x} \mathbf{y}_{\text{tot}})$	evals of $\pi(\mathbf{x} \mathbf{y}_n)$	evals of $\pi(\mathbf{x} \mathbf{y}_{\text{tot}})$	in the lower layer
LAIS	$NT$	0	$NT$	✓
PLAIS	0	$NT$	$NT$	✓
RLAIS	$NT$	0	0	✗
PA-RLAIS	0	$NT$	$NT$	✗
—	—	cheaper	—	—
CLAIS can be also combined with the other schemes above for building cheaper denominators.				

## 7 Data subset selection by PLAIS

Let us consider the use of partial posteriors in the upper layer and the temporal denominator in the weighting scheme in the lower layer. We will employ effective sample size (ESS) measures as a way of distinguishing the performance of each partial posterior, and subsequently, the importance of the corresponding subset of data. Namely, the goal is to find the most representative minibatch of data.

Furthermore, when the data is conditionally independent given the parameter vector, we also show in Sect. 7.2 how we can leverage the use of this most representative minibatch in order to produce an approximate complete posterior which is far less costly to evaluate than the true  $\bar{\pi}$ . Thus, this approximate and cheaper posterior (using only one minibatch) could be employed in further statistical studies. The ESS expressions try to measure the efficiency of IS as compared to the ideal case where we can sample independently from  $\bar{\pi}$  [30, 31]. Some examples of ESS measures are provided in Table 5.

Table 5: Selection of the mini-batch.

- **Compute the Effective Sample Size (ESS) measures:**

$$\text{ESS}(n) = \frac{1}{\sum_{t=1}^T \tilde{w}_{n,t}^2}, \quad \text{or} \quad \text{ESS}(n) = \frac{1}{\max_{t=1, \dots, T} \tilde{w}_{n,t}},$$

(note that  $1 \leq \text{ESS} \leq N$ ) where

$$w_{n,t} = \frac{\pi(\mathbf{x}_{n,t} | \mathbf{y}_{\text{tot}})}{\frac{1}{T} \sum_{\tau=1}^T q_{n,\tau}(\mathbf{x}_{n,t} | \boldsymbol{\mu}_{n,\tau})}, \quad \tilde{w}_{n,t} = \frac{w_{n,t}}{\sum_{t=1}^T w_{n,t}}.$$

- **Ranking:** Rank the minibatches - partial posteriors according to the  $\text{ESS}(n)$ ; the “best” minibatch is

$$n^* = \arg \max_n \text{ESS}(n).$$

## 7.1 ESS associated of each partial posterior

Assume we have run the PLAIS algorithm with independent parallel chains in upper layer, and using the temporal denominator in the lower layer. For each partial posterior, we have obtained the set  $\{\mathbf{x}_{n,t}\}_{t=1}^T$  with weights

$$w_{n,t} = \frac{\pi(\mathbf{x}_{n,t} | \mathbf{y}_{\text{tot}})}{\frac{1}{T} \sum_{\tau=1}^T q_{n,\tau}(\mathbf{x}_{n,t} | \boldsymbol{\mu}_{n,\tau})}, \quad \tilde{w}_{n,t} = \frac{w_{n,t}}{\sum_{t=1}^T w_{n,t}}, \quad t = 1, \dots, T. \quad (18)$$

We now compute the effective sample size  $\text{ESS}(n)$  using one of the formula in Table 5. Assuming that the  $n$ -th chain has converged, the value  $\text{ESS}(n)$  attempts to inform us about how close is  $\bar{\pi}_n$  to the optimal proposal, i.e., to  $\bar{\pi}$ . In this sense,  $\text{ESS}(n)$  measures the quality of the batch  $\mathbf{y}_n$  to imitate the whole data set  $\mathbf{y}_{\text{tot}}$ . Hence, the best minibatch is

$$n^* = \arg \max_n \text{ESS}(n). \quad (19)$$

Obtaining this subset of data,  $\mathbf{y}_{n^*}$ , can be useful for different purposes, e.g., see next section.

## 7.2 Obtaining an approximate complete posterior

Assume we have divided the data  $\mathbf{y}_{\text{tot}}$  in  $N$  batches of approximately equal size  $K_n \approx K$  for  $n = 1, \dots, N$ , that the batches are conditional independent and form a partition of the whole data set  $\mathbf{y}_{\text{tot}}$ , i.e.,

$$L(\mathbf{y}_{\text{tot}} | \mathbf{x}) = \prod_{n=1}^N L(\mathbf{y}_n | \mathbf{x}). \quad (20)$$

In this setting, the complete posterior can be factorized as follows

$$\bar{\pi}(\mathbf{x}|\mathbf{y}_{\text{tot}}) \propto L(\mathbf{y}_{\text{tot}}|x)g(\mathbf{x}) = \prod_{n=1}^N L(\mathbf{y}_n|\mathbf{x})g(\mathbf{x})^{\frac{1}{N}} \quad (21)$$

$$= \prod_{n=1}^N \pi_n(\mathbf{x}|\mathbf{y}_n), \quad (22)$$

that is, it is proportional to the product of partial posteriors  $\pi_n$ 's. This shows that, for  $\pi_n$  to have the same scale than the complete  $\pi$ , we would need to repeat it  $N$  times.

**Inflated partial posteriors.** As in [32], we can define *inflated partial posterior* by taking a powered likelihood function without making changes to the prior. The  $n$ -th inflated partial posterior is

$$\tilde{\pi}_n(\mathbf{x}|\mathbf{y}_n) \propto [\bar{\pi}_n(\mathbf{x}|\mathbf{y}_n)]^{\frac{D_Y}{K}} = [\bar{\pi}_n(\mathbf{x}|\mathbf{y}_n)]^N \quad (23)$$

$$\propto L(\mathbf{y}_n|\mathbf{x})^N g(\mathbf{x}). \quad (24)$$

The inflated partial posterior  $\tilde{\pi}_n$  has roughly the same magnitude as the complete posterior.

**Approximated complete posterior.** The inflated partial posterior corresponding to the most representative minibatch  $\mathbf{y}_{n^*}$  (see previous section), serves as a cheap approximation of complete posterior,

$$\tilde{\pi}_{n^*}(\mathbf{x}|\mathbf{y}_{n^*}) \approx \bar{\pi}(\mathbf{x}|\mathbf{y}_{\text{tot}}), \quad (25)$$

where  $\tilde{\pi}_{n^*}(\mathbf{x}|\mathbf{y}_{n^*})$  is an approximated complete posterior. We can use  $\tilde{\pi}_{n^*}(\mathbf{x}|\mathbf{y}_{n^*})$  in variety of ways, e.g., to carry out further Monte Carlo runs using  $\tilde{\pi}_{n^*}(\mathbf{x}|\mathbf{y}_{n^*})$  instead of  $\bar{\pi}(\mathbf{x}|\mathbf{y}_{\text{tot}})$ , hence reducing the computational cost.

## 8 Numerical experiments

In this Section, we test the performance of some of the algorithms described in this work. We have considered three scenarios. The first experiment consists in estimating the posterior of a toy observation model with synthetic data. Here, we aim to investigate the effect of using partial posteriors in the upper layer, as compared to using the full posterior. We also test the performance of the recycling strategy. In the second experiment, we consider a bimodal example where we compare the application of HMC-LAIS algorithms against only HMC with twice the number of iterations. In the third experiment, we apply the Gibbs-LAIS scheme to a regression problem on the daily deaths by COVID in Italy. Some related codes are available at [https://github.com/FLlorente/LAIS\\_extensions](https://github.com/FLlorente/LAIS_extensions).

### 8.1 First experiment

In our first example, we generate 50 observations,  $\mathbf{y}_{\text{tot}} = \{y_i\}_{i=1}^{50}$ , from the following observation model

$$y_i = \exp(-\alpha t_i) \sin(\beta t_i) + v_i$$

where the values  $\alpha$  and  $\beta$  were fixed at 0.1 and 2, respectively. This model is a very simplified version of a more complex astronomical model (see Example 3 in [17]). The error terms  $v_i$  were independently generated from a Gaussian,  $\mathcal{N}(0, 0.1^2)$ . For this model, we take  $\mathbf{x} = [\alpha, \beta]^\top$  and set a uniform density over the rectangle  $[0, 10] \times [0, 2\pi]$  as prior density for  $\mathbf{x}$ . The goal is to investigate the use of partial posteriors in the LAIS framework when computing  $\mathbb{E}[\mathbf{x}|\mathbf{y}_{\text{tot}}]$ ,  $\text{var}[\mathbf{x}|\mathbf{y}_{\text{tot}}]$  (marginal variances) and  $Z = p(\mathbf{y}_{\text{tot}})$ . By using a very thin grid over the space, we are able to calculate the true values, obtaining  $\mathbb{E}[\mathbf{x}|\mathbf{y}_{\text{tot}}] = [0.1, 2]^\top$ ,  $\text{var}[\mathbf{x}|\mathbf{y}_{\text{tot}}] = [6.88 \cdot 10^{-5}, 8.38 \cdot 10^{-5}]^\top$  and  $Z = 3.03 \cdot 10^{-15}$ . We compute the MSE in estimating those quantities with the following methods: (a) LAIS, (b) PLAIS, and (c) PA-RLAIS.

The number of total evaluations of the posterior is  $E = 2000$ . For all the methods, the upper layer consists of  $N$  independent random walk Metropolis algorithms with Gaussian proposals. Here, PLAIS and PA-RLAIS differ from LAIS in that, instead of the full posterior, each of the  $N$  chains targets a different partial posterior (with the same number of data  $K_n$  for all  $n$ ). In the lower layer, one sample was drawn from each Gaussian proposal. The covariance matrix of all the Gaussian proposals was set to  $2I_2$ . Here, PA-RLAIS differs from LAIS and PLAIS, in that no sample is drawn in this second stage, but all samples are recycled from the chains in the upper layer. We tested several combinations of number of chains,  $N$ , and length of the chains,  $T$ , in a manner that the product  $TN$  was constant and equal to  $\frac{E}{2} = 1000$ . More specifically, we tested the values  $N \in \{1, 2, 5, 10, 25, 50\}$ . Note that PLAIS and PA-RLAIS only evaluate the complete posterior in the lower layer, and hence have a cost of  $\frac{E}{2}$  (see Sect. 6.1). In each simulation the partial posteriors were created by choosing randomly  $K_n$  data, with  $K_n \in \{5, 10\}$ . Figure 1 depicts the model with a subset of the observations generated from it. The orange dots are the observations chosen to construct the partial posterior in one simulation with  $K_n = 5$ . Finally, in all the methods, the initial mean vectors were drawn from the prior, i.e.,  $\boldsymbol{\mu}_{n,0} \sim \mathcal{U}([0, 10] \times [0, 2\pi])$ , for all  $n$ . The results are averaged over 500 independent simulations.

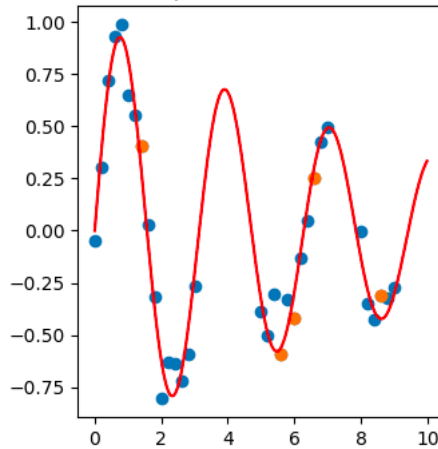


Figure 1: Model and data generated. The solid line is the function that defines the model, and the blue dots are the observations generated from it.

In Figure 2, we show the obtained results. In both graphics, we see the behavior of the MSE when  $N$  changes. The solid line corresponds to the usual LAIS implementation where we use all

the data available for the computation of the likelihood in the upper layer. The dashed lines show the behavior of the errors when partial posteriors are considered in the upper layer. The left side shows the case  $K_n = 5$  for all  $n$ , while, on the right side, we show  $K_n = 10$  for all  $n$ . In both graphics, it can be seen that PLAIS and PA-RLAIS outperform the results of standard LAIS, for the values of  $N$  considered. Hence, in this simple example, using partial posteriors improves the performance of the algorithms. For all methods, the error tends to grow after certain optimal  $N$ . However, the methods that use partial posteriors show better performance, as compared to standard LAIS, when  $N$  increases, that is, when there is more number of shorter chains. This can be due to the fact that the partial posteriors are wider, and hence easier to explore in a small number of iterations. Also in both cases, the errors of PLAIS and PA-RLAIS are rather similar, although, as expected, PLAIS outperforms PA-RLAIS.

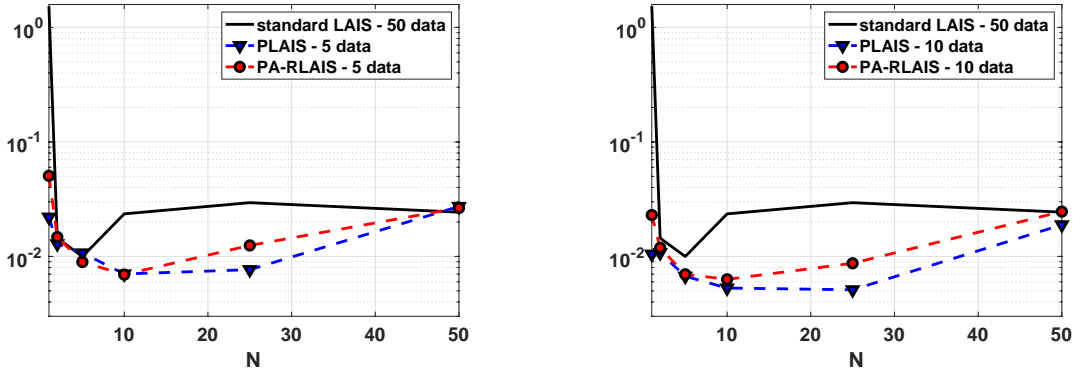


Figure 2: MSE of the algorithms for distinct numbers of data in the partial posterior. In the left side, we show the error using 5 data points. In the right side, we show the error using 10 data points.

## 8.2 HMC importance samplers vs HMC algorithms

For the next experiment, we consider  $\bar{\pi}(\mathbf{x})$  which consists of an equally-weighted mixture of two Gaussian pdfs. The Gaussians pdfs are located at  $[0, 0]^\top$  and  $[-4, 4]^\top$ , respectively. The covariance matrix of both is  $\Sigma = [4, 3; 4, 3]$ . Here, it is straightforward to calculate the true values for the quantities of interest: the expected value is  $[-2, 2]^\top$ , the variances are  $[8, 8]$  and the covariance is  $-1$ . In this simple example, we aim to test the performances of HMC-LAIS algorithms in estimating these quantities. The goal is to compare their performances against only using HMC algorithms. The error measure we employ is the averaged Mean Squared Error (MSE) in estimating those quantities: expected value of  $\bar{\pi}(\mathbf{x})$  (2 quantities), and covariance matrix of  $\bar{\pi}(\mathbf{x})$  (3 quantities).

The budget is  $E = 2400$  target evaluations. We consider HMC algorithms with kinetic energy using a Gaussian distribution with covariance matrix equal to  $2\mathbf{I}$ , and test the following values for step length and path length  $\{(0.25, 1), (0.5, 1), (1, 3), (1, 5)\}$ . In the lower layer, we also consider Gaussian proposals with covariance matrix equal to  $2\mathbf{I}$ . Here, we compare the performance of

three deterministic-mixture weighting schemes: spatial, temporal and complete.

For setting the number of chains,  $N$ , and the number of iterations,  $T$ , we follow the same rules as for the previous experiment. We kept constant the product  $NT = \frac{E}{2} = 1200$  and vary  $N$  within  $\{2,3,4,6,8,10,12,16,20,25,30,40,50,60,100\}$ . For a fair comparison, when we only consider HMC algorithms, the  $N$  chains were run for  $2T$  iterations each (i.e. twice number of iterations than the HMC algorithms in the upper layer of the HMC-LAIS algorithms), so that the final number of target evaluations is  $2NT = E = 2400$ . The initial mean vectors were chosen uniformly within the square  $[-10, 10]^2$ . The results were averaged over 500 independent simulations.

In Figure 3, we show the MSE of the HMC and HMC-LAIS algorithms, with three weighting schemes, as a function of  $N$ . Recall that, for every  $N$ , the HMC algorithms were run for twice number of iterations, i.e., they were run for  $2T$  iterations, in order to have the same number of target evaluations. Each figure corresponds to a different choice of step and path lengths in the HMC algorithms.

**First main observation.** We can observe that the LAIS schemes (except some few specific cases) always outperform the HMC algorithms.

**Second main observation.** It is important to remark the excellent and robust performance provided by HMC-LAIS with the *complete* denominator, regardless the parameters of HMC chains (in the upper layer) used and the number of chains  $N$ . In fact, HMC-LAIS algorithm with complete denominator clearly outperforms the rest of techniques, providing the smallest error and remaining constant for all  $N$  and all HMC parameters.

**Other considerations.** The error of HMC is smallest when  $N$  is close to the minimum (i.e. when the chains are longer), and gets worse as  $N$  increases since, consequently, the chains become shorter and cannot explore properly the two modes. Interestingly, even in the best scenario, the results show that the error of HMC is always greater than the one provided by HMC-LAIS algorithms with temporal and complete denominators. Namely, even when HMC works best, it is better to run it for half number of iterations and then use it within the LAIS framework with a temporal or complete denominator.

**Spatial vs Temporal.** The performance of the temporal and spatial denominators behave in an opposite manner. The error corresponding to the spatial denominator is worse when  $N$  is small. In fact, the biggest error is always when  $N$  is minimum. As  $N$  increases, the performance greatly improves. Indeed, it rapidly beats HMC and its performance matches that of the complete weighting scheme for large  $N$ . Conversely, in the temporal denominator, the best results are always achieved when  $N$  is minimum, since in this case, the chain length  $T$  is maximum. As  $N$  increases, the performance of the temporal denominator worsens, but in a slower fashion than the corresponding error of the HMC algorithms.

In this experiment, the spatial denominator seems to outperform the temporal denominator for more values of  $N$ . This means that the mixture of spatial proposals is usually better than the mixture of temporal proposals. For some value  $N_*$ , both weighting schemes provide the same results. Only for values  $N \leq N_*$ , the temporal denominator is better than the spatial denominator. Namely, if  $T$  is not sufficiently big ( $T \geq \frac{E}{2N_*}$ ), the temporal denominator does not pay off, as compared to the spatial denominator. In fact, for  $N > 50$ , the spatial denominator can be considered as a compressed version of the complete denominator, i.e., it provides almost the same

performance but with a smaller number of components (recall that the complete denominator has  $\frac{E}{2} = 1200$  mixture components).

**Compressed schemes.** We have also tested the performance of compressed LAIS (CLAIS), where a compression technique is applied to the  $NT$  proposals from the upper layer (see Sect. 5.2). Here, we have run a clustering algorithm with  $\{3, 21, 50, 200\}$  clusters to obtain the compressed denominators. In Figure 4, we show the error of these schemes against the three previous weighting schemes and HMC. With the proposed compression scheme, we see that the performance is very close to that of the complete denominator and it is insensitive to the choice of number of clusters and  $N$ . For moderately low  $N$ , CLAIS outperforms LAIS with spatial denominator. However, as  $N$  increases, the spatial denominator matches the performance of CLAIS, i.e., the spatial denominator is also a very efficient way of compressing the  $NT$  proposals as discussed above. Finally, in Figure 5 we display the computation time of CLAIS versus the compression level  $\eta$ , which is  $\eta = 0$  when there is no compression at all ( $M = NT$ , i.e. the maximum number of clusters), and  $\eta = 1 - \frac{1}{NT}$  when we have  $M = 1$  clusters.

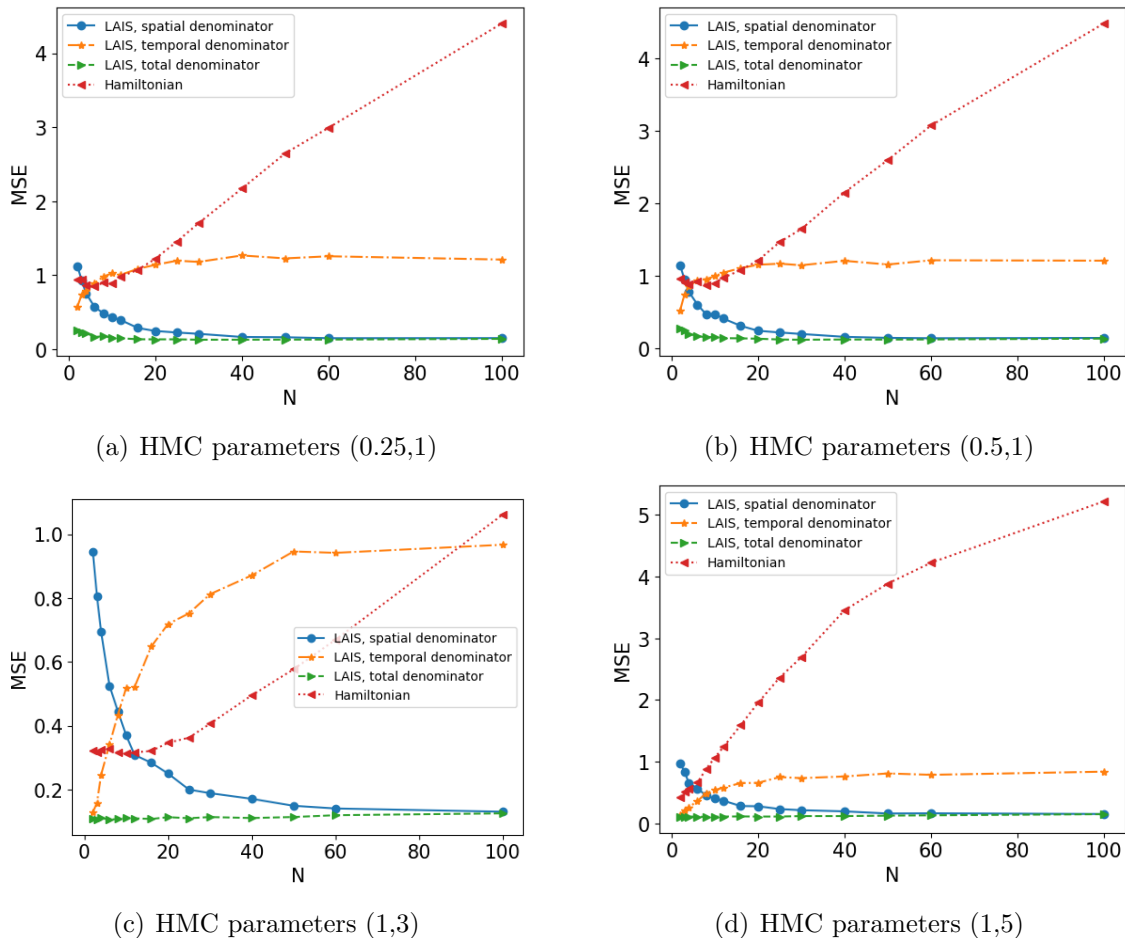


Figure 3: MSE in estimation obtained by HMC-LAIS and HMC versus  $N$ , with the same number of evaluations of the posterior  $E = 2400$  (hence, the HMC chains have twice the length of the HMC chains used in the upper layer of HMC-LAIS). Each figure corresponds to a different choice of step and path lengths in the HMC algorithms.

### 8.3 Experiment with COVID-19 data

We consider the number of daily deaths caused by SAR-CoV-2 in Italy from 18 February 2020 to 6 July 2020 as the dataset. We denote the values of daily deaths as  $\mathbf{y} = [y_1, \dots, y_{D_y}]^\top$ . Let  $t_i$  denote the  $i$ -th day, we model each observation as

$$y_i = f(t_i) + e_i, \quad i = 1, \dots, D_y = 140,$$

where  $f$  is the function that we aim to approximate and  $e_i$ 's are independent Gaussian realizations with zero means and variance  $\sigma_e^2$ . We consider the approximation of  $f$  at some  $t$  as a weighted sum of  $M$  localized basis functions,

$$f(t) = \sum_{m=1}^M \rho_m \psi(t | \mu_m, h, \nu),$$

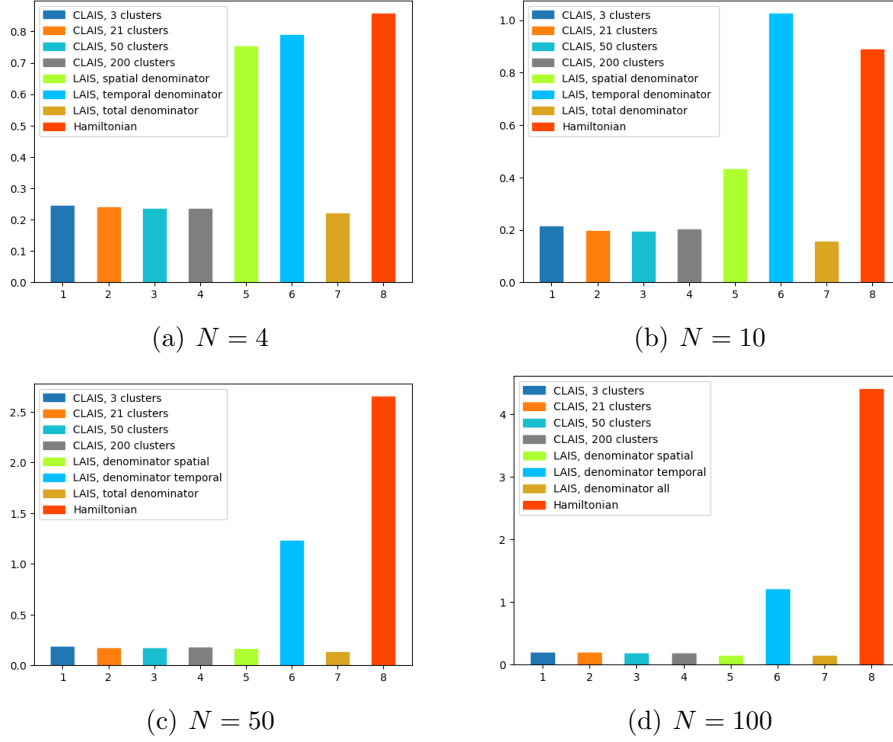


Figure 4: MSE of CLAIS with different values of  $M \in \{3, 21, 50, 200\}$ , compared with LAIS with different denominators and parallel HMC chains (with twice lengths with respect to the LAIS schemes, in order to have the same number of posterior evaluations  $E = 2400$  for all methods).

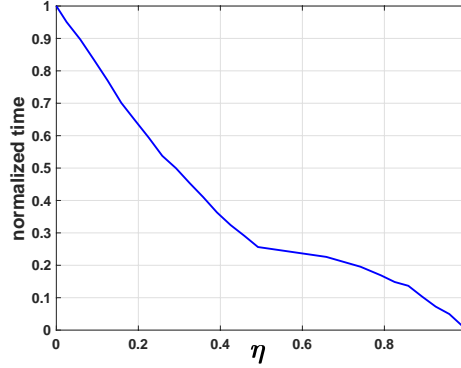


Figure 5: Normalized computational time versus compression level  $\eta$ , where  $\eta = 1 - \frac{M}{NT}$ , and  $M$  is the number of clusters.

where  $\psi(t|\mu_m, h)$  is  $m$ -th basis located at  $\mu_m$  with bandwidth  $h$ . Let also be  $\nu$  an index denoting the type of basis. We consider  $M \in \{1, \dots, D_y\}$ , then  $1 \leq M \leq D_y$ . When  $M = D_y$ , the model becomes a Relevance Vector Machine (RVM), and the interpolation of all data points (maximum overfitting, with zero fitting error) is possible [33]. We study 2 possible kinds of basis (i.e.,  $\nu = 1, 2$ ):

Gaussian ( $\nu = 1$ ), and Laplacian ( $\nu = 2$ ). After fixing  $\nu$  and  $M$ , we select the locations  $\{\mu_m\}_{m=1}^M$  as a uniform grid in the interval  $[1, D_y]$  (recall that  $D_y = 140$ ). Hence, by knowing  $\nu$  and  $M$ , the locations  $\{\mu_m\}_{m=1}^M$  are given.

We define the vector of coefficients  $\boldsymbol{\rho} = [\rho_1, \dots, \rho_M]^\top$ . Let also  $\boldsymbol{\Psi}$  be a  $D_y \times M$  matrix with elements  $[\boldsymbol{\Psi}]_{i,m} = \psi(t_i|\mu_m, h)$  for  $i = 1, \dots, D_y$  and  $m = 1, \dots, M$ . Then, the observation equation in vector form is

$$\mathbf{y} = \boldsymbol{\Psi}\boldsymbol{\rho} + \mathbf{e},$$

where  $\mathbf{e} \sim \mathcal{N}(\mathbf{0}, \sigma_e^2 \mathbf{I}_{D_y})$  is a  $D_y \times 1$  vector of noise, where  $\mathbf{I}_{D_y}$  is the  $D_y \times D_y$  identity matrix. Therefore, the likelihood function will be

$$\ell(\mathbf{y}|\boldsymbol{\rho}, h, \sigma_e, \nu, M) = \mathcal{N}(\mathbf{y}|\boldsymbol{\Psi}\boldsymbol{\rho}, \sigma_e^2 \mathbf{I}_N).$$

We assume a Gaussian prior density over the vector of coefficients  $\boldsymbol{\rho}$ , i.e.,  $g(\boldsymbol{\rho}|\lambda) = \mathcal{N}(\boldsymbol{\rho}|\mathbf{0}, \boldsymbol{\Sigma}_\rho)$ , where  $\boldsymbol{\Sigma}_\rho = \lambda \mathbf{I}_M$  and  $\lambda > 0$ . Therefore, the complete set of parameters to infer is  $\{\boldsymbol{\rho}, \nu, M, h, \lambda, \sigma_e\}$ . The conditional posterior of  $\boldsymbol{\rho}$  given the rest of parameters is also Gaussian,

$$\bar{\pi}(\boldsymbol{\rho}|\mathbf{y}, \lambda, h, \sigma_e, \nu, M) = \frac{\ell(\mathbf{y}|\boldsymbol{\rho}, h, \sigma_e, \nu, M)g(\boldsymbol{\rho}|\lambda)}{p(\mathbf{y}|\lambda, h, \sigma_e, \nu, M)} = \mathcal{N}(\boldsymbol{\rho}|\boldsymbol{\mu}_{\boldsymbol{\rho}|\mathbf{y}}, \boldsymbol{\Sigma}_{\boldsymbol{\rho}|\mathbf{y}}),$$

and a likelihood marginalized w.r.t.  $\boldsymbol{\rho}$  is available in closed-form,

$$p(\mathbf{y}|\lambda, h, \sigma_e, \nu, M) = \mathcal{N}(\mathbf{y}|\mathbf{0}, \boldsymbol{\Psi}\boldsymbol{\Sigma}_\rho\boldsymbol{\Psi}^\top + \sigma_e^2 \mathbf{I}_N). \quad (26)$$

For further details see [33]. Now, we assume  $g_\lambda(\lambda)$ ,  $g_h(h)$ ,  $g_\sigma(\sigma_e)$  are folded-Gaussian priors over  $h, \lambda, \sigma_e$ , defined on  $\mathbb{R}_+ = (0, \infty)$  with location and scale parameters  $\{0, 100\}$ ,  $\{0, 400\}$  and  $\{1.5, 9\}$ , respectively. Then, we study the following posterior marginalized w.r.t.  $\boldsymbol{\rho}$  and conditioned to  $\mu, M$ ,

$$\bar{\pi}(\lambda, h, \sigma_e|\mathbf{y}, \nu, M) = \frac{1}{p(\mathbf{y}|\nu, M)} p(\mathbf{y}|\lambda, h, \sigma_e, \nu, M) g_\lambda(\lambda) g_h(h) g_\sigma(\sigma_e),$$

Finally, we want to compute the marginal likelihood, i.e.,

$$p(\mathbf{y}|\nu, M) = \int_{\mathbb{R}_+^3} p(\mathbf{y}|\lambda, h, \sigma_e, \nu, M) g_\lambda(\lambda) g_h(h) g_\sigma(\sigma_e) d\lambda dh d\sigma_e. \quad (27)$$

Furthermore, assuming a uniform probability mass  $p(M = i) = \frac{1}{D_y}$  as prior over  $M$ , we have  $p(M|\mathbf{y}, \nu) = \frac{p(\mathbf{y}|\nu, M)p(M)}{p(\mathbf{y}|\nu)} \propto \frac{1}{D_y} p(\mathbf{y}|\nu, M)$ . We can marginalize out  $M$  obtaining

$$p(\mathbf{y}|\nu) = \frac{1}{D_y} \sum_{M=1}^{D_y} p(\mathbf{y}|\nu, M), \quad \text{for } \nu = 1, 2. \quad (28)$$

Considering also a uniform prior over  $\nu$ , we can obtain the marginal posterior  $p(\nu|\mathbf{y}) \propto \frac{1}{2} p(\mathbf{y}|\nu)$ . **Goal.** Our purpose is: (a) to make inference regarding the parameters of the model  $\{\lambda, h, \sigma_e\}$ , (b) approximate  $Z = p(\mathbf{y}|\nu, M)$ , (c) study the posterior  $p(M|\mathbf{y}, \nu)$ . We also study the marginal

posterior  $p(\nu|\mathbf{y})$  for  $\nu = 1, 2$ .

**Methods.** For approximating  $p(\mathbf{y}|\nu, M)$ , for  $M = 1, \dots, D_y$ , and  $p(\nu|\mathbf{y})$ , we first apply a Naive Monte Carlo (NMC) method with  $10^4$  samples. We apply also a Gibbs-LAIS scheme with a MH-within-Gibbs sampler in the upper layer. More specifically, we employ an interpolative piecewise constant function as proposal in the MH scheme to draw from the full-conditionals (considering 2 internal steps) [26]. Hence, in the upper layer, we obtain a unique Markov chain ( $N = 1$ ) of  $\boldsymbol{\mu}_t = [\lambda_t, h_t, \sigma_{e,t}]$  for  $t = 1, \dots, T$ . We set  $T = 5000$ , hence also 5000 samples drawn in the lower layer and used in estimators. The total number of evaluations of the posterior is  $2T = 10^4$  for both, NMC and Gibbs-LAIS schemes.

**Results.** With both methods, We obtain that MAP estimator of  $M$  is  $M^* = 8$ . In Figure 6, we show the fitting obtained with  $M = 8$  bases and the parameter estimations provided by the Gibbs-LAIS scheme. Thus, a first conclusion is that the results obtained with models such as RVMs and Gaussian Processes (GPs) (both having  $M = 140$  [33]) can be approximated in a very good way with a much more scalable model, as our model here with only  $M = 8$  [33]. Regarding the marginal posterior  $p(\nu|\mathbf{y})$ , we can observe the results in Table 6. With the results provided by both schemes, we should prefer slightly the Laplacian basis. These considerations are reasonable after having a look at Figure 6.

Table 6: The approximate marginal posterior  $p(\nu|\mathbf{y})$  with different techniques.

Method	$p(\nu = 1 \mathbf{y})$	$p(\nu = 2 \mathbf{y})$
NMC	0.4831	0.5169
Gibbs-LAIS	0.4930	0.5070

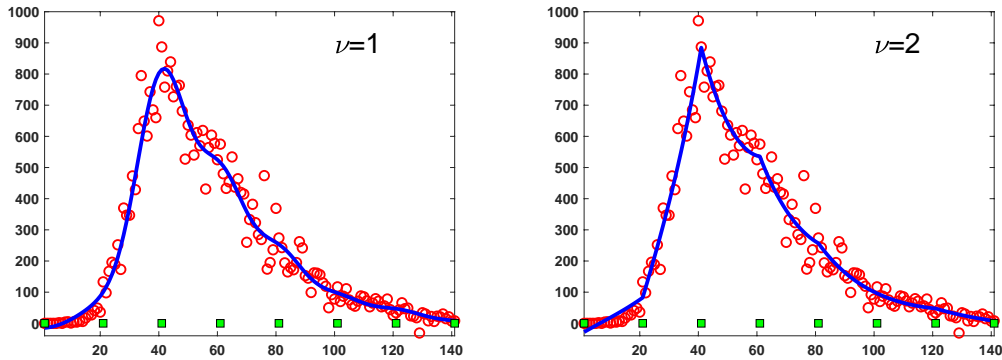


Figure 6: Best fit with 8 bases with different types of basis,  $\nu = 1, 2$ . The circles represent the analyzed data and the squares show the positions of the bases.

## 9 Conclusions

LAIS is a flexible framework for designing AIS algorithms. In the upper layer, MCMC algorithms drive the adaptation of the location parameters of the proposal densities, which are then used in the lower layer, where a MIS scheme is performed. In this paper, we have introduced variants in the LAIS framework in order to improve the overall performance and reduce computational costs. Specifically, we propose that the MCMC algorithms in the upper layer address different partial posteriors (i.e., posteriors of subsets of data) to improve the mixing of the chains due to the data-tempering effect, and at the same time, reducing the costs of the upper layer. We also proposed the use of sophisticated MCMC algorithms, such as HMC and advanced Gibbs techniques, in the upper layer. The resulting algorithms inherit the good mixing properties and additionally provide an estimator of the marginal likelihood. We discussed general strategies to reduce the cost of the lower layer based on recycling and compression. For certain setups, we are able to recycle all the samples from the upper layer and form the final estimator without further evaluations of the posterior. Finally, we have also shown the application of our schemes to the problem of minibatch selection. Numerical experiments show that these variants outperform standard applications of LAIS and other benchmark algorithms.

## References

- [1] C. P. Robert and G. Casella, *Monte Carlo Statistical Methods*. Springer, 2004.
- [2] J. S. Liu, *Monte Carlo Strategies in Scientific Computing*. Springer, 2004.
- [3] A. Doucet, N. de Freitas, and N. Gordon, Eds., *Sequential Monte Carlo Methods in Practice*. New York (USA): Springer, 2001.
- [4] W. J. Fitzgerald, “Markov chain Monte Carlo methods with applications to signal processing,” *Signal Processing*, vol. 81, no. 1, pp. 3–18, January 2001.
- [5] M. Hong, M. F. Bugallo, and P. M. Djuric, “Joint model selection and parameter estimation by population monte carlo simulation,” *Selected Topics in Signal Processing, IEEE Journal of*, vol. 4, no. 3, pp. 526–539, 2010.
- [6] P. M. Djurić, B. Shen, and M. F. Bugallo, “Population Monte Carlo methodology a la Gibbs sampling,” in *EUSIPCO*, 2011.
- [7] P. D. Moral, A. Doucet, and A. Jasra, “Sequential Monte Carlo samplers,” *Journal of the Royal Statistical Society: Series B (Statistical Methodology)*, vol. 68, no. 3, pp. 411–436, 2006.
- [8] L. Martino, V. Elvira, D. Luengo, and J. Corander, “Layered adaptive importance sampling,” *Statistics and Computing*, vol. 27, pp. 599–623, 2017.
- [9] V. Elvira, L. Martino, D. Luengo, and M. F. Bugallo, “Generalized Multiple Importance Sampling,” *Statistical Science*, vol. 34, no. 1, pp. 129–155, 2019.

- [10] E. Veach and L. Guibas, “Optimally combining sampling techniques for Monte Carlo rendering,” *In SIGGRAPH 1995 Proceedings*, pp. 419–428, 1995.
- [11] V. Elvira, L. Martino, D. Luengo, and M. F. Bugallo, “Heretical multiple importance sampling,” *IEEE Signal Processing Letters*, vol. 23, no. 10, pp. 1474–1478, 2016.
- [12] L. Martino and V. Elvira, “Compressed Monte Carlo with application in particle filtering,” *Information Sciences*, vol. 553, pp. 331–352, 2021.
- [13] Y. El-Laham, L. Martino, V. Elvira, and M. F. Bugallo, “Efficient adaptive multiple importance sampling,” in *2019 27th European Signal Processing Conference (EUSIPCO)*. IEEE, 2019, pp. 1–5.
- [14] F. Llorente, L. Martino, D. Delgado, and J. Lopez-Santiago, “Marginal likelihood computation for model selection and hypothesis testing: an extensive review,” *arXiv preprint arXiv:2005.08334*, 2020.
- [15] D. P. Liu, Q. T. Zhang, and Q. Chen, “Structures and performance of noncoherent receivers for unitary space-time modulation on correlated fast-fading channels,” *IEEE Transactions Vehicular Technology*, vol. 53, no. 4, pp. 1116–1125, July 2004.
- [16] F. Liang, C. Liu, and R. Carroll, *Advanced Markov Chain Monte Carlo Methods: Learning from Past Samples*. England: Wiley Series in Computational Statistics, 2010.
- [17] F. Llorente, L. Martino, D. Delgado, and G. Camps-Valls, “Deep importance sampling based on regression for model inversion and emulation,” *arXiv preprint arXiv:2010.10346*, 2020.
- [18] D. J. Earl and M. W. Deem, “Parallel tempering: Theory, applications, and new perspectives,” *Physical Chemistry Chemical Physics*, vol. 7, no. 23, pp. 3910–3916, 2005.
- [19] R. M. Neal, “Annealed importance sampling,” *Statistics and computing*, vol. 11, no. 2, pp. 125–139, 2001.
- [20] S. L. Scott, A. W. Blocker, F. V. Bonassi, H. A. Chipman, E. I. George, and R. E. McCulloch, “Bayes and big data: The consensus Monte Carlo algorithm,” in *EFaBBayes 250th conference*, vol. 16, 2013.
- [21] W. Neiswanger, C. Wang, and E. Xing, “Asymptotically exact, embarrassingly parallel MCMC,” *arXiv:1311.4780*, pp. 1–16, 21 Mar. 2014.
- [22] S. Livingstone and G. Zanella, “On the robustness of gradient-based MCMC algorithms,” *arXiv preprint arXiv:1908.11812*, vol. 1, no. 1.1, pp. 1–2, 2019.
- [23] W. R. Gilks, N. G. Best, and K. K. C. Tan, “Adaptive Rejection Metropolis Sampling within Gibbs Sampling,” *Applied Statistics*, vol. 44, no. 4, pp. 455–472, 1995.

- [24] R. Meyer, B. Cai, and F. Perron, “Adaptive rejection Metropolis sampling using Lagrange interpolation polynomials of degree 2,” *Computational Statistics and Data Analysis*, vol. 52, no. 7, pp. 3408–3423, March 2008.
- [25] L. Martino, J. Read, and D. Luengo, “Independent doubly adaptive rejection Metropolis sampling within Gibbs sampling,” *IEEE Transactions on Signal Processing*, vol. 63, no. 12, pp. 3123–3138, 2015.
- [26] L. Martino, H. Yang, D. Luengo, J. Kannianen, and J. Corander, “The FUSS algorithm: a Fast Universal Self-tuned Sampler within Gibbs,” *viXra:1405.0263*, 2014.
- [27] W. R. Gilks, G. O. Roberts, and E. I. George, “Adaptive direction sampling,” *Journal of the Royal Statistical Society: Series D (The Statistician)*, vol. 43, no. 1, pp. 179–189, 1994.
- [28] I. Schuster and I. Klebanov, “Markov Chain Importance Sampling? a highly efficient estimator for MCMC,” *Journal of Computational and Graphical Statistics*, pp. 1–9, 2020.
- [29] D. Rudolf and B. Sprungk, “On a Metropolis–Hastings importance sampling estimator,” *Electronic Journal of Statistics*, vol. 14, no. 1, pp. 857–889, 2020.
- [30] L. Martino, V. Elvira, and F. Louzada, “Effective sample size for importance sampling based on discrepancy measures,” *Signal Processing*, vol. 131, pp. 386–401, 2017.
- [31] V. Elvira, L. Martino, and C. P. Robert, “Rethinking the effective sample size,” *arXiv preprint arXiv:1809.04129*, 2018.
- [32] R. Entezari, R. V. Craiu, and J. S. Rosenthal, “Likelihood inflating sampling algorithm,” *Canadian Journal of Statistics*, vol. 46, no. 1, pp. 147–175, 2018.
- [33] L. Martino and J. Read, “A joint introduction to Gaussian Processes and Relevance Vector Machines with connections to Kalman filtering and other kernel smoothers,” *Information Fusion*, vol. 74, pp. 17–38, 2021.

## Appendices

### A Hierarchical interpretation of the random walk Metropolis-Hastings (MH) algorithm

Consider a target density  $\pi(\mathbf{x}) \propto \bar{\pi}(\mathbf{x})$  and a random-walk proposal pdf  $q(\mathbf{x}|\mathbf{x}_{t-1}, \mathbf{C}) = q(\mathbf{x} - \mathbf{x}_{t-1}|\mathbf{0}, \mathbf{C})$ , where  $\mathbf{x}_{t-1}$  the current state of the chain and  $\mathbf{C}$  is a covariance matrix. One

transition of the MH algorithm is summarized by 1. Draw  $\mathbf{x}'$  from a proposal pdf  $q(\mathbf{x}|\mathbf{x}_{t-1}, \mathbf{C})$ .  
 2. Set  $\mathbf{x}_t = \mathbf{x}'$  with probability

$$\alpha = \min \left[ 1, \frac{\pi(\mathbf{x}') q(\mathbf{x}_{t-1}|\mathbf{x}', \mathbf{C})}{\pi(\mathbf{x}_{t-1}) q(\mathbf{x}'|\mathbf{x}_{t-1}, \mathbf{C})} \right]$$

otherwise set  $\mathbf{x}_t = \mathbf{x}_{t-1}$  (with probability  $1 - \alpha$ ). There are two well-known general classes of proposal pdf: independent proposal  $q$  (independent from the current state), and random walk proposal,  $q(\mathbf{x}|\mathbf{x}_{t-1}, \mathbf{C})$ , as we considered above. The use of a random walk proposal  $q(\mathbf{x} - \mathbf{x}_{t-1}|\mathbf{0}, \mathbf{C})$  is often preferred due to its explorative behavior, since it relocates the proposal at the current state of the chain at each iteration. See Figure 7(a)-(b), for an example. As a consequence, the common wisdom is that this approach is more robust with respect to the choice of the tuning parameters. Below, we provide some further arguments explaining the success of the random walk approach.

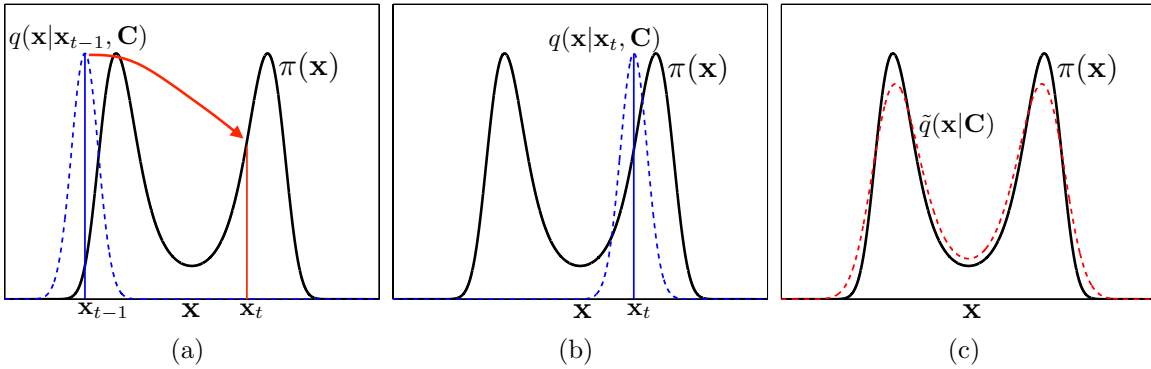


Figure 7: Graphical representation of the equivalent proposal of a random-walk proposal in a MH method. A bimodal target pdf  $\pi(\mathbf{x})$  is shown in solid line. The proposal densities are depicted in dashed lines. (a) A proposal pdf  $q(\mathbf{x}|\mathbf{x}_{t-1}, \mathbf{C}) = q(\mathbf{x} - \mathbf{x}_{t-1}|\mathbf{0}, \mathbf{C})$  at the iteration  $t - 1$ , and the next state of the chain  $\mathbf{x}_t$ . (b) The proposal pdf  $q(\mathbf{x}|\mathbf{x}_t, \mathbf{C}) = q(\mathbf{x} - \mathbf{x}_t|\mathbf{0}, \mathbf{C})$  at the  $t$ -th iteration. (c) The equivalent independent proposal pdf  $\tilde{q}_{MH}(\mathbf{x}|\mathbf{C})$  is represented in dashed line.

We can provide a hierarchical interpretation in the same fashion on LAIS. Let us assume a "burn-in" length  $T_b - 1$ . Hence, considering an iteration  $t \geq T_b$ , we can assert  $\mathbf{x}_t \sim \bar{\pi}(\mathbf{x})$ . It implies that the random walk generating process is equivalent, for  $t \geq T_b$ , to the following hierarchical procedure: (a) draw a location parameter  $\boldsymbol{\mu}'$  from  $\bar{\pi}(\boldsymbol{\mu})$ , (b) draw  $\mathbf{x}'$  from  $q(\mathbf{x}|\boldsymbol{\mu}', \mathbf{C})$ . Therefore, for  $t \geq T_b$ , the probability of proposing a new sample (i.e., the equivalent proposal) can be written as

$$\begin{aligned} \tilde{q}_{MH}(\mathbf{x}|\mathbf{C}) &= \int_{\mathcal{X}} q(\mathbf{x}|\mathbf{x}_{t-1}, \mathbf{C}) \bar{\pi}(\mathbf{x}_{t-1}) d\mathbf{x}_{t-1}, \\ &= \int_{\mathcal{X}} q(\mathbf{x} - \mathbf{x}_{t-1}|\mathbf{0}, \mathbf{C}) \bar{\pi}(\mathbf{x}_{t-1}) d\mathbf{x}_{t-1}, \quad \text{for } t \geq T_b, \end{aligned} \quad (29)$$

since  $\mathbf{x}_{t-1} \sim \bar{\pi}(\mathbf{x}_{t-1})$  after a burn-in period,  $t \geq T_b$ , and  $\mathbf{x}_{t-1}$  represents the location parameter of  $q$ . The function  $\tilde{q}_{MH}(\mathbf{x}|\mathbf{C})$  is an equivalent independent proposal pdf corresponding to a random

walk generating process within an MCMC method (after the "burn-in" period). See Figure 7(c) for an example of  $\tilde{q}_{MH}$ .

Clearly, this interpretation has no direct implications for practical purposes, since we are not able to draw directly from the target  $\bar{\pi}$ . However, it is useful for clarifying the main advantage of the random walk approach, i.e., that the equivalent proposal  $\tilde{q}_{MH}$  is a better choice than an independent proposal roughly tuned by the user with non-optimal parameters. In fact, as an example, Eq. (29) ensures that the equivalent proposal  $\tilde{q}_{MH}(\mathbf{x}|\mathbf{C})$  has a fatter tails than the target  $\bar{\pi}$ . Indeed, the random walk generating procedure includes indirectly certain information about the target: denoting  $\mathbf{X} \sim \tilde{q}_{MH}(\mathbf{x}|\mathbf{C})$ ,  $\mathbf{Z} \sim q(\mathbf{x}|\mathbf{0}, \mathbf{C})$  and  $\mathbf{M} \sim \bar{\pi}(\mathbf{x})$ , we have

$$E[\mathbf{X}] = E[\mathbf{M}], \quad \Sigma_X = \mathbf{C} + \Sigma_M,$$

where  $E[\mathbf{M}]$  and  $\Sigma_M$  are the mean and covariance matrix of the target pdf  $\bar{\pi}(\mathbf{x})$ .